The Neurochip-2: An Autonomous Head-Fixed Computer for Recording and Stimulating in Freely Behaving Monkeys

Stavros Zanos, Andrew G. Richardson, Larry Shupe, Frank P. Miles, and Eberhard E. Fetz

***Abstract*—The Neurochip-2 is a second generation, battery-powered device for neural recording and stimulating that is small enough to be carried in a chamber on a monkey's head. It has three recording channels, with user-adjustable gains, filters, and sampling rates, that can be optimized for recording single unit activity, local field potentials, electrocorticography, electromyography, arm acceleration, etc. Recorded data are stored on a removable, flash memory card. The Neurochip-2 also has three separate stimulation channels. Two "programmable-system-on-chips" (PSoCs) control the data acquisition and stimulus output. The PSoCs permit flexible real-time processing of the recorded data, such as digital filtering and time-amplitude window discrimination. The PSoCs can be programmed to deliver stimulation contingent on neural events or deliver preprogrammed stimuli. Access pins to the microcontroller are also available to connect external devices, such as accelerometers. The Neurochip-2 can record and stimulate autonomously for up to several days in freely behaving monkeys, enabling a wide range of novel neurophysiological and neuroengineering experiments.**

***Index Terms*—Brain–computer interface (BCI), neural recording, neural stimulation, primate.**

I. Introduction

NEUROPHYSIOLOGICAL experiments in nonhuman primates typically involve monitoring neural activity during intermittent recording sessions in a controlled laboratory setting. Likewise, brain–computer interface (BCI) experiments, which decode neural activity in real-time to control a device, generally use rack-mounted equipment, limiting a subject's experience with the BCI to several hours a day and within a restricted environment. While such laboratory experiments have advantages, both neurophysiological and neuroengineering research could benefit from a portable system that would allow neural recording and electrical stimulation to be performed continuously during free behavior for extended periods of time.

Manuscript received December 08, 2010; revised March 11, 2011; accepted April 27, 2011. Date of publication May 31, 2011; date of current version August 10, 2011. This work was supported in part by National Institutes of Health (NIH) under Grant NS12542 and Grant RR00166, in part by the Life Sciences Discovery Fund, in part by the Christopher and Dana Reeve Foundation, in part by the American Heart Association under award 0825963G, and in part by an award from the Institute of Translational Health Sciences (ITHS). S. Zanos and A. G. Richardson contributed equally to this work.

S. Zanos and E. E. Fetz are with the Department of Physiology and Biophysics and with the Washington National Primate Research Center, University of Washington, Seattle, WA 98195 USA.

A. G. Richardson is with the Department of Physiology and Biophysics, University of Washington, Seattle, WA 98195 USA.

L. Shupe and F. P. Miles are with the Washington National Primate Research Center, University of Washington, Seattle, WA 98195 USA.

Color versions of one or more of the figures in this paper are available online at http://ieeexplore.ieee.org.

Digital Object Identifier 10.1109/TNSRE.2011.2158007

Several portable systems for neural recording have been developed [1]–[8]. Some of them include closed-loop stimulation capability [8]–[12]. The original "Neurochip-1" previously developed in this laboratory [11] was a battery-powered device small enough to be carried inside a chamber on a monkey's head. It could record neuronal activity on one channel (0.5–5 kHz passband; 11.7 kS/s; 8 bit resolution) and electromyographic (EMG) activity on two other channels (20 Hz–1 kHz passband; 2 kS/s; 8 bit resolution). The 8 MB on-board memory was sufficient to store up to 27 h of continuous data by calculating and storing spike rates and average EMG over user-defined time bins, interspersed with intermittent samples of raw data to confirm recording quality. The microcontroller could be programmed to detect action potentials of single neurons with a user-defined time-amplitude window discriminator. These capabilities permitted long-term recordings of neuronal and EMG activity during free behavior and natural sleep [13]. Neurochip-1 could also deliver stimulation contingent on recorded activity, supporting novel types of BCI experiments. The spike-triggered stimulation produced by the Neurochip operating in this closed-loop mode was used to strengthen synaptic connections between two sites in the brain [9]. It could also be used to provide artificial recurrent connections, for example between the motor cortex and spinal cord [10] or between motor cortex and paralyzed muscles [14]. The ability to deliver activity-dependent stimulation has also been demonstrated with nonportable instrumentation [15]–[17]. While such potential neurorehabilitation paradigms could be performed with conventional laboratory equipment, their success in producing lasting changes lies in the ability to deliver activity-dependent stimulation for extended periods of time in an unconstrained environment.

The Neurochip-1 was designed to implement a recurrent BCI (R-BCI) that utilizes neural spikes as input signals and delivers intracortical electrical stimuli as its output [9]. The majority of the portable systems for neural recording developed in other laboratories, with few exceptions (e.g., [18]), are optimized for recording spiking activity. Despite considerable scientific and clinical experience with cortical neuronal activity in BCI applications, there is interest in using alternative, more robust and less invasive brain signals to control BCI systems [19]. For example, local field potentials (LFPs) appear to have greater long-term stability than neuronal spikes in chronic intracortical recordings, and electrocorticography (ECoG) electrodes provide less invasive access to brain signals while maintaining high temporal and spatial resolution. In addition, novel motor rehabilitation paradigms would benefit from the ability of a BCI

system to deliver electrical stimuli to multiple different sites of the nervous system. For example, the direct cortical control of functional electrical stimulation demonstrated primarily with laboratory instrumentation [14] could be implemented continuously, during natural behavior, through cortically-triggered stimulation of multiple muscles or sites in the spinal cord.

With these considerations in mind, the next generation of portable BCI systems should meet several requirements that would make them more useful for both basic neurophysiology research and neuroengineering applications. They should be able to record a variety of different neural signals; to perform various signal processing and feature extraction algorithms in real time; to interface easily with external input and output devices; and to deliver electrical stimuli to multiple sites of the nervous system or muscles. Neurochip-1, as well as the rest of the available portable BCI systems, lack many of these requirements. The second generation of the Neurochip, called Neurochip-2, was designed to meet as many of these requirements as possible. Below we describe the architecture of Neurochip-2, highlighting the important differences and improvements over the original version, and demonstrate its performance on the bench and in several new experimental paradigms.

II. Neurochip-2 Architecture

Like the original Neurochip, Neurochip-2 is housed in a custom-fabricated titanium casing that is attached to the animal's skull (Fig. 1(a); see also [11]). The device is powered by rechargeable batteries stored in the casing lid. A version of the Neurochip-2 with a high-voltage stimulator consists of four circuit boards (39 g), powered by two batteries, with a total weight of 204 g (Fig. 1(b), right). A more compact version of the Neurochip-2 with lower stimulator output has three circuit boards (36 g), powered by one battery, with a total weight of 145 g (Fig. 1(b), left). Neurochip-2 has six main components: the analog front-end, the microcontroller system, the memory system, the stimulator system, the powering, and the interface [Fig. 2(a)]. A Matlab-based graphic user interface (GUI) running on a personal computer is used to upload settings to the Neurochip-2 and download and display data (Fig. 3). Recordings are stored on a removable flash memory card with up to 2-GB capacity. Communication between the computer and Neurochip-2 is achieved through a serial cable or wirelessly via an infrared (IR) data link.

The main differences between Neurochip-1 and Neurochip-2 are summarized in Table I and described below. Complete schematics for these units are available online.[1]

A. Analog Front-End

The analog front-end implements three independent differential channels (A, B, and C). In the first stage of each channel, the AC-coupled input signals are amplified by a pair of operational amplifiers configured for a $\times 50$ gain and a selectable single-pole, low-frequency cutoff. All gain and filter switching is performed by analog switches controlled by the microcontrollers. The second stage uses an instrumentation amplifier configured for a gain of $\times 20$ or $\times 100$ and a selectable single-pole,

[1]http://auk.wanprc.org/nc2

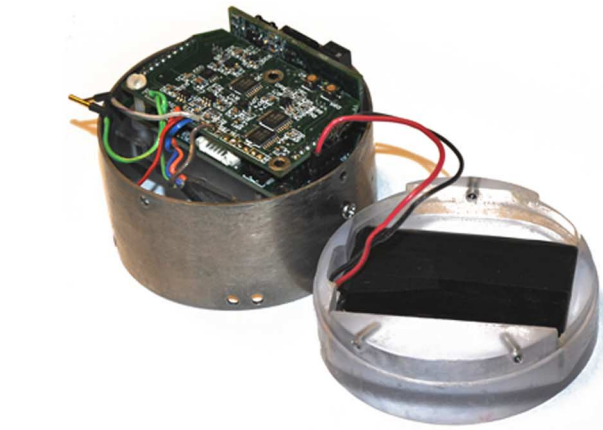

(a)

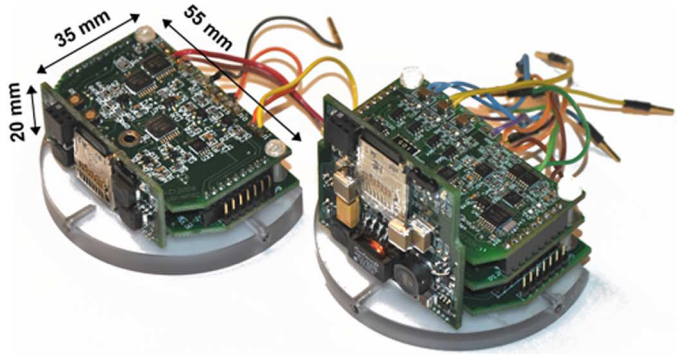

(b)

Fig. 1. (A) Neurochip-2 inside the titanium casing (attached via nylon screws to a polycarbonate base, not visible). The battery is housed in the polycarbonate lid, shown to the right. (B) The two versions of the Neurochip-2: a compact, lower output current version (left) and a larger, high output current version (right). The gold access pins (bottom right of boards) allow connections to external devices and access four data channels on PSoC-B.

low-cut frequency. To suppress artifacts produced by stimulation, all gains can be transiently reduced to one; this greatly reduces the probability that filter capacitors will be charged nonlinearly during a stimulation event and hastens signal recovery. The output range of the analog amplification is ± 1.3 V relative to tissue ground.

For channels A and C, the combined analog low-frequency cutoff can be switched between a low value (10 Hz, for recording field potentials), and a high value (500 Hz, for recording action potentials). The high-frequency cutoff is 7.5 kHz. For channel B, the analog passband is fixed at 10 Hz to 2.5 kHz. Additional user-defined digital filtering is performed by the microcontroller system (see Section II-B). All three channels share the same tissue ground.

B. Microcontroller System

Like Neurochip-1, the microcontroller system consists of two "Programmable System-on-Chip" (PSoC) devices (CY8C29466, Cypress Semiconductor, San Jose, CA). PSoC-A digitizes input from channel A and controls the stimulator system. PSoC-B digitizes input from channels B and C. Channel A data collected on PSoC-A is streamed to a buffer on PSoC-B, which then writes the data from all three channels to a binary file on the memory card. The two PSoCs communicate with each other via an asynchronous serial bus [Fig. 2(a)].

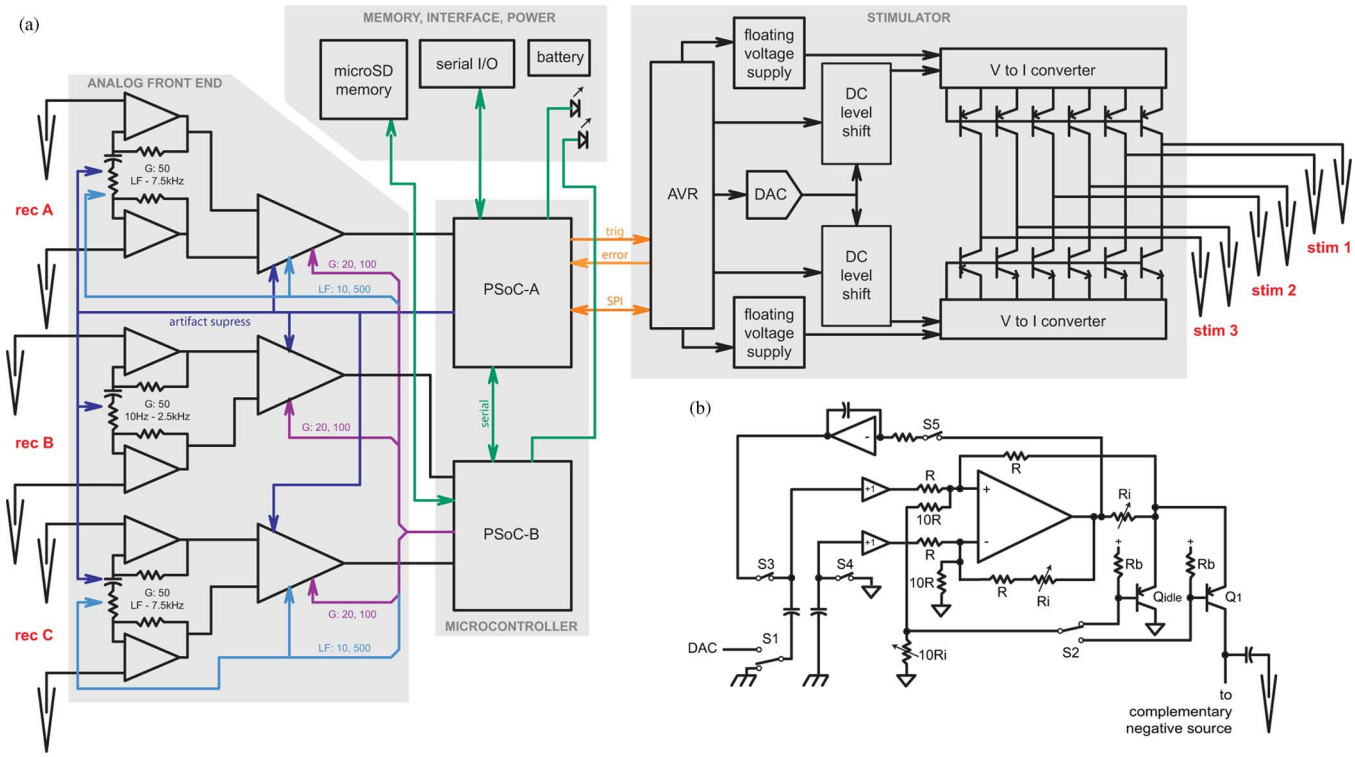

Fig. 2. (A) Block diagram of the major Neurochip-2 components and signal routing. G: gain, LF: low-pass filter cutoff (Hz), PSoC: programmable system-on-chip, SPI: serial peripheral interface, AVR: Atmel AVR microcontroller, DAC: digital-to-analog converter. Connections between the battery and active components are not shown. (B) Circuit diagram of one of the "V to I converter" blocks.

Each PSoC features a number of modules that can be configured using proprietary software (PSoC Designer IDE, Cypress Semiconductor Corporation) to perform a variety of tasks such as analog-to-digital conversion (ADC), amplification, filtering, and other signal processing. In Neurochip-2, ADC blocks digitize input signals with 8-bit resolution at a user-specified sampling rate (256 S/s to 24 kS/s). Additional switched capacitor and digital modules perform signal processing operations in real-time, including bandpass filtering, signal squaring, averaging over intervals, and time-amplitude window discrimination. The time-amplitude discriminator consists of two user-defined windows following a threshold crossing that can be set to detect action potentials of single neurons, or LFP/ECoG waves of specific frequencies, or increases in power in specific frequency ranges (e.g., with the discrimination windows operating on a filtered and squared version of the input field potential signal). Acceptance pulses can be further processed and stored to on-board memory. Upon detection of criterion events, PSoC-A can trigger the delivery of electrical stimuli through the stimulator system. This PSoC can be programmed to turn the triggered stimulation on and off at set intervals. The PSoC can also trigger the stimulator independently of discrimination events. For example, it can be configured to deliver stimuli at regular preset intervals, or at pseudorandom intervals at a set average rate. Finally, the PSoC can be programmed to switch gains and filters on a channel at regular intervals during the recording, to capture both single unit activity and LFP from the same electrode at different times. All of the user-defined settings for the microcontroller system are specified and uploaded via a Matlab-based GUI (Fig. 3).

C. *Memory System*

The amplified, filtered, and digitized signals can be stored on a 2-GB microSD flash memory card. The memory card can be manually removed from the Neurochip-2 and placed in a USB drive to download the recorded data to a personal computer. The 2-GB memory is sufficient to hold approximately 93 h of continuous 8-bit LFP/ECoG/EMG data on three channels sampled at 2 kS/s, or 35 h of continuous 8-bit data from a single channel of unit activity sampled at 12 kS/s plus two channels of LFP/ECoG/EMG data sampled at 2 kS/s. Interleaved storage of raw data and binned averages can be implemented via the Matlab GUI to extend the duration of these recordings, in which case the chosen proportions and battery life become the limiting factors. Use of memory cards with capacity greater than 2 GB (e.g., microSDHC cards) is incompatible with the deployed PSoC version.

D. *Stimulator System*

The stimulator system in Neurochip-2 comes in two versions, depending on current intensity and voltage compliance requirements. The regular version (Fig. 1(b), left) has an output compliance of ± 15 V and can deliver biphasic, constant-current pulses in the range of 10–200 μA through typical high-impedance microelectrodes. The "high compliance voltage" (HCV) version (Fig. 1(b), right) delivers constant-current pulses within a ± 50 V compliance range. We have found this range adequate for reaching the 0.5–5 mA threshold for evoking motor output with relatively low impedance electrodes (~ 10 kΩ at 1 kHz) placed at the cortical surface.

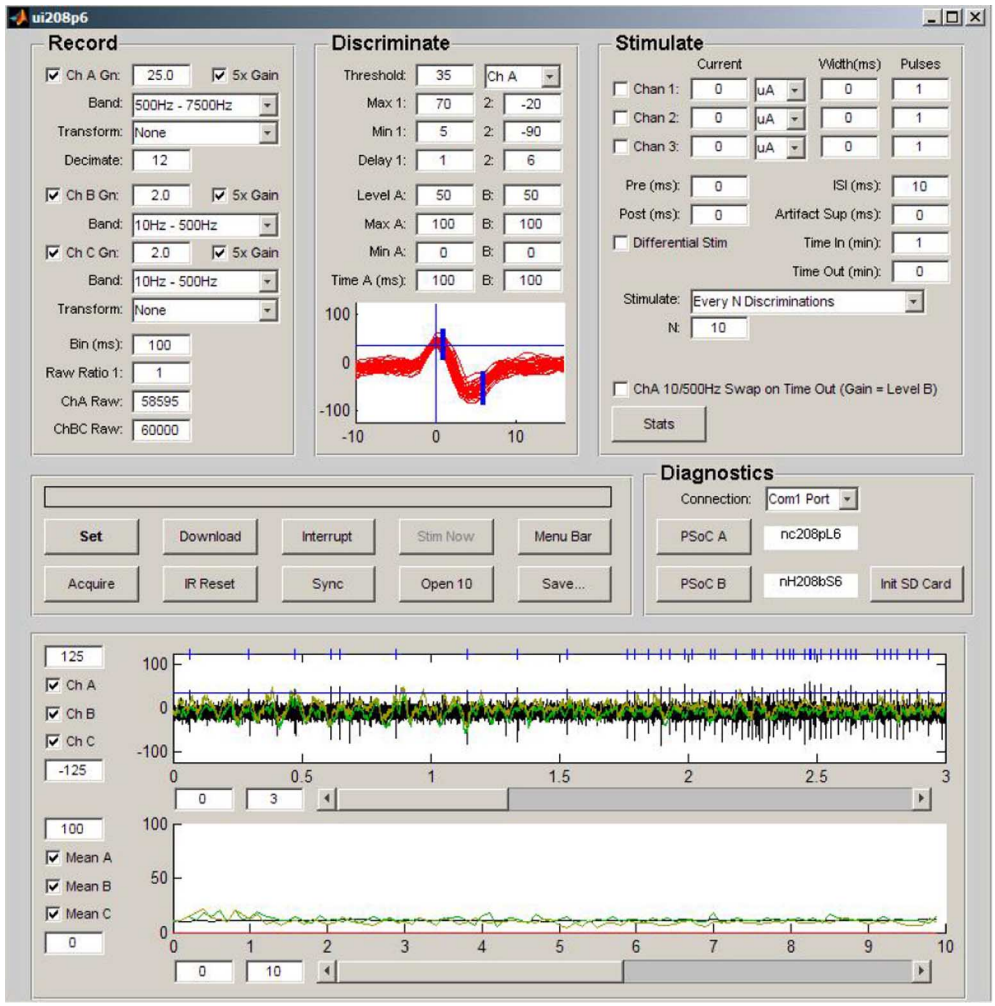

Fig. 3. Matlab-based graphical user interface on a PC. Upper bank of windows shows uploadable parameters for recording, spike discrimination and stimulation. Middle window illustrates action potentials recorded on channel A (red traces) and discriminated via a threshold (horizontal line) and two time-amplitude windows. Window below shows 3 s of raw data from three intracortical electrodes: neuronal activity on channel A (black trace), and wide-band (10–500 Hz) LFPs on channels B and C (green and yellow traces). Blue lines indicate spike times detected by window discriminator. Lowest window shows binned activity over 10-s interval.

TABLE I
COMPARISON OF THE NEUROCHIP-1, NEUROCHIP-2, AND A COMPARABLE PORTABLE SYSTEM (HERMES-D [3])

Feature	Neurochip-1	Neurochip-2	Hermes-D
Enclosure	55x50x30 mm^3	63x63x30 mm^3	38x38x51 mm^3
Power consumption	40-120 mW	284-420 mW	142 mW
Recording channels	1 unipolar & 2 bipolar	3 unipolar/bipolar	32 unipolar
ADC resolution	8 bit	8 bit	12 bit
On-board data storage	8 MB	2000 MB	N/A (wireless)
Adjustable sampling rate/filters	no	yes	no
Access pins to microcontroller	no	yes	N/A
Stimulation channels	1 unipolar	3 unipolar/bipolar	0
Stimulation compliance voltage	±15V	±15V (reg), ±50V (HCV)	N/A
Duration of continuous operation	≤ 60 hours†	≤ 48 hours†	33 hours

†depends on the operating mode.

In contrast to the single unipolar stimulation channel in Neurochip-1, both stimulator versions in Neurochip-2 feature three bipolar stimulation channels. Each channel pair can have a unique set of stimulus parameters, including current intensity, pulse width, number of pulses per trigger, pulse train frequency, and trigger-to-stimulus latency. All stimulation channels share programmable high-output impedance current sources, precluding simultaneous delivery of multiple pulses. However, switching times between different channels are sufficiently brief ($< 70\ \mu s$) to provide near-simultaneous and precisely timed sequential stimulation.

The HCV stimulator is implemented with two modified Howland current sources driving high-voltage bipolar transistors to minimize power consumption. Essentially all of the quiescent current consumed flows within the floating 4-V supplies, except while delivering a stimulus pulse. At idle, the integrator associated with S3 and S5 feedback sets the output bias current to ~ 100 nA through pseudo-output transistor Q_{idle} into the

floating positive ground [Fig. 2(b)], compensating for any offset voltage in the Howland opamp. The only high-voltage current loss is the < 50 nA Icbo of each output transistor. To deliver a positive current pulse, switches S3-5 open, S2 is set to the desired output transistor, and S1 is switched to the DAC output voltage [Fig. 2(b)]. The capacitors couple the DAC voltage level to the Howland subcircuit, which ensures that the same voltage appears across the output current-setting resistor Ri connected to Q1's emitter. 0.1% resistors are used to ensure accurate matching with the complementary negative source in delivering biphasic output pulses. The low-impedance, common-base input ensures that the Howland circuit will be stable even without trimming the resistor network. Transistor base current is corrected by feedback to the Howland circuit, ensuring accurate current output and increasing the already high output resistance. MOSFET output transistors were not used since they require larger floating supply voltages, have high output capacitance (diverting output current from the electrodes), and have poorly specified leakage currents approaching minimum stimulation levels. The output impedance of this circuit is limited primarily by the output transistor and wiring capacitance.

The stimulator for the standard Neurochip-2 uses a simpler dual Howland circuit to provide differential current output capability. The lower compliance range allows the use of an ordinary op-amp as the current source and a low-power analog switch as the output electrode selector. A low-frequency feedback path around the current source ensures that the output coupling capacitors do not get charged from current associated with small offset voltages without significantly degrading the high output impedance.

E. Power

The electronic circuits are powered by one (for regular stimulator version) or two (HCV version) rechargeable, 3.6-V lithium-ion batteries of approximately 1.75-Ah capacity (UBP103450, Ultralife Batteries). A $+5$ V generator is needed for the second stage instrumentation amplifiers. The standard Neurochip-2 uses a dual voltage converter (Linear Technology LT1945) to generate ± 15 V relative to tissue ground. The HCV version uses a Texas Instruments TPS61045 with a CoilCraft HP1-0059 transformer to create the floating 4 V supplies, and a Maxim 1771 to generate the ± 15–55 V supply. All other nonstimulator circuitry operate directly from the battery.

F. Interface

Communicating and interfacing with the Neurochip-2 is more versatile than in Neurochip-1. In addition to the serial and IR links, which can be used to program Neurochip-2 and download data from it, Neurochip-2 has a set of pins [Fig. 1(b)] that give access to many different levels of the analog front-end and the microcontroller system, increasing the flexibility of both input and output operations. Analog or digital signals can be registered directly on the PSoC, in parallel to neural signals routed through the analog front-end. At the same time, the output of the analog front-end can be routed to external devices, such as an oscilloscope or an audio speaker, essentially rendering the Neurochip as a mini headstage amplifier. The same can be done with the output of the microcontroller system. Acceptance pulses from the time-amplitude discriminator can be used to trigger an external stimulator or to control external devices in real time.

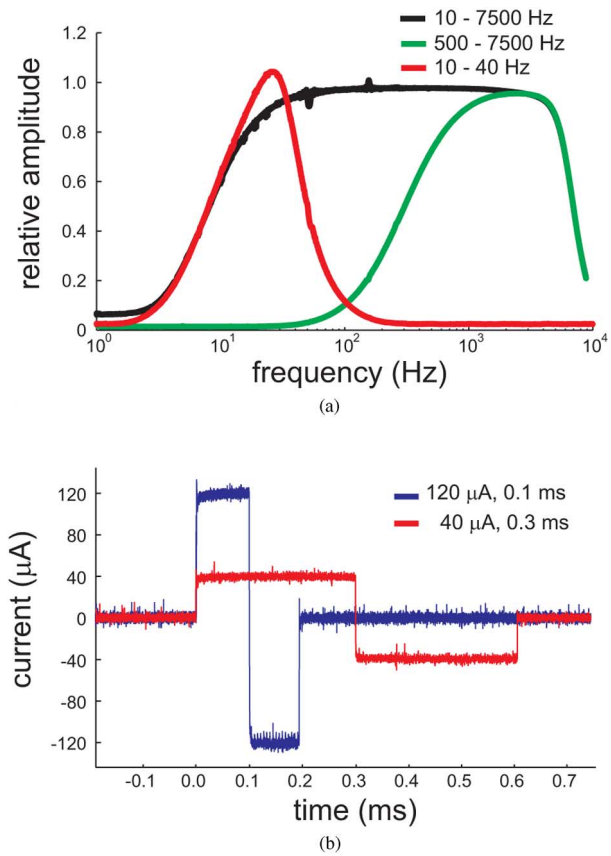

Fig. 4. Bench testing results. (A) Measured frequency response for three different filter settings of channel A operating at maximum sampling rate (24 kS/s). (B) Measured output of the stimulator for two different intensities and pulse widths.

III. Bench Testing

We performed a number of bench-top tests to ensure that the Neurochip-2 was operating as intended. First, the input-referred noise, measured with grounded inputs at high gain ($\times 20\,000$) and wide passband (10 Hz to 7.5 kHz), was 2.7 μVrms. This is lower than the thermal noise, at this bandwidth, of an electrode with impedance greater than 60 kΩ. The noise floor was not appreciably affected by simultaneous recording and stimulating.

Second, the programmable filters were evaluated with constant-amplitude sine wave frequency sweeps input into each channel. Fig. 4(a) shows the relative change in amplitude as a function of frequency for three example filter settings for channel A operating at maximum sampling rate (24 kS/s). The intended filter cutoffs, indicated in the figure legend, were closely approximated in the measured frequency response. Unlike the first two settings that relied solely on the analog front-end filters, the 10–40 Hz setting (Fig. 4(a), red line) required the use of a digital filter implemented in the PSoC switched capacitor blocks. The slight increase in midband gain for the 10–40 Hz filter setting was a result of the passband ripple associated with the particular Chebyshev design we used for the switched-capacitor filter. Similar frequency responses were obtained for channels B and C.

TABLE II
POWER CONSUMPTION OF THE NEUROCHIP-2

Operating mode	Power (mW)	
	Regular	HCV
1. Idling	116	144
2. Recording		
2a. chA,B,C @ 2 kS/s	284	308
2b. chA @ 24 kS/s, chB,C @ 2 kS/s	304	324
3. Recording + Discriminating		
3a. 2b + 10 discrim/s	328	332
3b. 2b + 100 discrim/s	364	376
4. Recording + Stimulating*		
4a. 2b + 4 stim/s	352	365
4b. 2b + 10 stim/s	388	401
5. Recording + Discriminating + Stimulating*		
5a. 3a + 10 stim/s	412	420

* 100 μA through a 100 kΩ resistor.

Third, we evaluated the ability of the stimulator system to deliver biphasic pulses with accurate amplitude and duration. Stimulus output was measured across a series resistor on a 1.25-GS/s digital oscilloscope. Two example output pulses produced by the regular (low compliance voltage) version of the stimulator are shown in Fig. 4(b). Again, the waveforms accurately follow the intended stimulus parameters indicated in the legend. A similarly high accuracy was observed for the HCV stimulator.

Fourth, the total power consumption of the Neurochip-2 was measured for several different operating modes, including recording, discriminating, and stimulating in various combinations. The results for the two versions of the stimulator are listed in Table II. The HCV version of Neurochip-2 consumed slightly more power than the regular version. But the power consumption for stimulation was comparable for the two versions when stimulating at the same intensity (100 μA) through the same load (100 kΩ).

IV. *In Vivo* TESTING

After verifying the functionality of Neurochip-2 on the bench, several experiments were conducted to demonstrate the performance of the system in freely behaving primates. In particular, these experiments evaluated many of the new features of the Neurochip-2: adjustable filters, greater data storage, access pins to the microcontroller, and high-intensity stimulation.

A. Methods

Two pigtailed macaques (*Macaca nemestrina*), R and X, were used for *in vivo* testing of the Neurochip-2. All surgical and experimental procedures were approved by the University of Washington Institutional Animal Care and Use Committee.

Monkey R received an intracortical, movable microwire array implant in the hand representation of the left precentral gyrus. The implant design and surgical technique have been described in detail previously [20]. Briefly, the implant consisted of 16 individually movable tungsten wires held inside polyamide guide tubes. After performing a left frontal craniotomy, a flap of dura was removed to reveal the left central sulcus and the electrode array was positioned along its anterior bank. The implant and the connectors were secured to the skull with acrylic cement and enclosed in a titanium casing that was also attached to the skull with cement and skull screws. Several of the skull screws were electrically connected and served as ground leads. To quantify motor behavior during the in-cage recording sessions, the macaque wore a 3-axis accelerometer (MMA7340LT, Freescale Semiconductor), powered by a 3 V lithium coin cell. The three analog outputs of the accelerometer were passed through a sum-of-absolutes circuit to give the resultant acceleration magnitude. This voltage was sent to a pair of access pins, bypassing the analog front-end, and digitized on one of the Neurochip-2 channels at 2 kS/s. The accelerometer was attached to the monkey's right forearm with medical tape and protected by a long-sleeve primate jacket. Wiring from the accelerometer was routed inside the jacket to a connector at the animal's back; that connector was subcutaneously wired to a second connector inside the titanium casing.

Monkey X was implanted with a subdural ECoG array (Ad-Tech Medical Instrument Corp., Racine, WI) over the hand representation of the left precentral gyrus. The array consisted of 32 platinum discs (1.5 mm exposed diameter) arranged in a 4×8 grid with 3-mm spacing. After a left frontal craniotomy, the dura was incised and retracted to reveal the left central sulcus. The array was placed on the pia overlying the precentral gyrus and covered by the dura and skull flap that was then secured with acrylic cement. Connectors were secured on the skull with cement and enclosed within the titanium casing. In a second surgery, multiple subcutaneously-routed EMG wires were implanted in eight muscles of the right arm. The connector for the EMG wires was secured inside the titanium casing.

Each experimental session began with the animal seated in a primate chair and brought into the lab. Neurochip-2 was then configured by entering the desired settings into the Matlab GUI (Fig. 3) and uploading them via the IR link. The animal was then returned to its cage, where it moved freely until being brought out the following day. Recorded data was downloaded from Neurochip-2 at the beginning of the next session.

An offline, time-frequency analysis was used to characterize the time course of field potential (LFP/ECoG) power throughout the duration of the in-cage recordings. Spectrograms of the signals were computed using the short-time Fourier transform with 1-s, Hamming-tapered windows, averaged over bins of 30-s duration. Relative power was then computed by dividing the absolute power by the mean marginal spectrum across all time bins.

B. Results

With Neurochip-2 the filters and gains on each channel can be independently adjusted to accommodate the characteristics of a variety of neural signals. Electrocorticographic (ECoG) signals are of particular interest since they could provide a less invasive and more robust trigger for activity-dependent stimulation to promote plasticity in the brain [9]. Fig. 5 shows an example of an ECoG signal recorded continuously for about 35 h from a subdural array in monkey X. A time-frequency analysis revealed correlates of the diurnal sleep pattern, with low-frequency activity (< 20 Hz) prominent during the night and a more subtle elevation of high-frequency activity (> 80 Hz) during the day (Fig. 5). At about 12:30 (point 3), the animal was sedated for an hour with ketamine (10 mg/kg). Sedation yielded a unique ECoG signature, consisting of bursts of oscillations at $\sim$40–50 Hz.

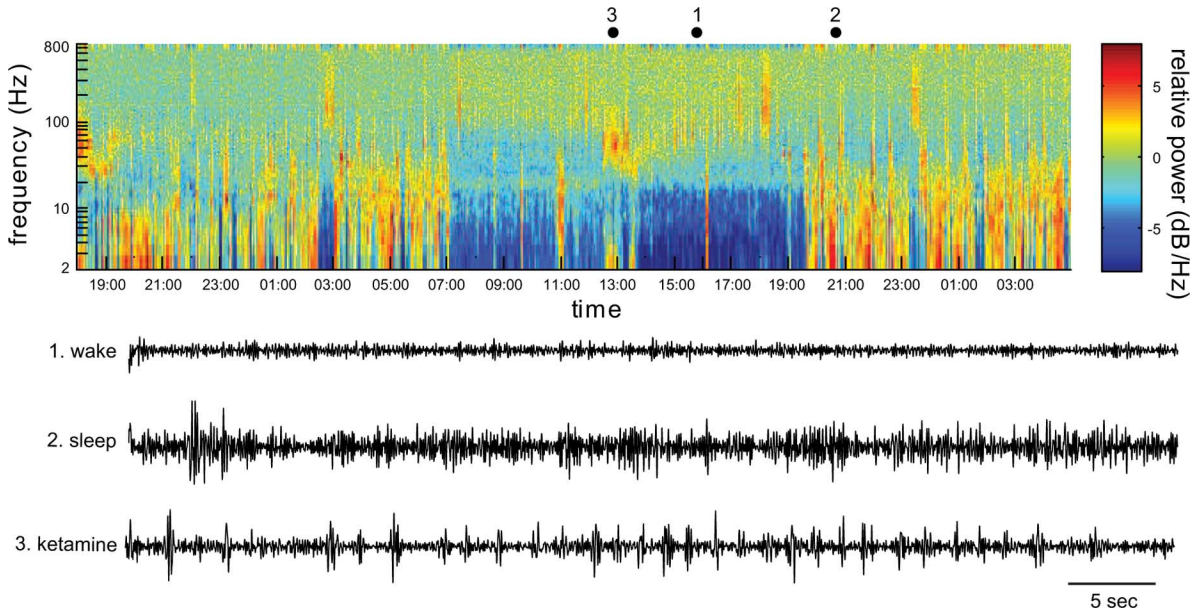

Fig. 5. Thirty-five-hour continuous ECoG recording from a cortical surface electrode over the precentral gyrus. The upper plot shows a spectrogram of the recording (power calibration at right). Three short segments of raw data are shown in the lower plots, corresponding to times indicated by the dots above the spectrogram.

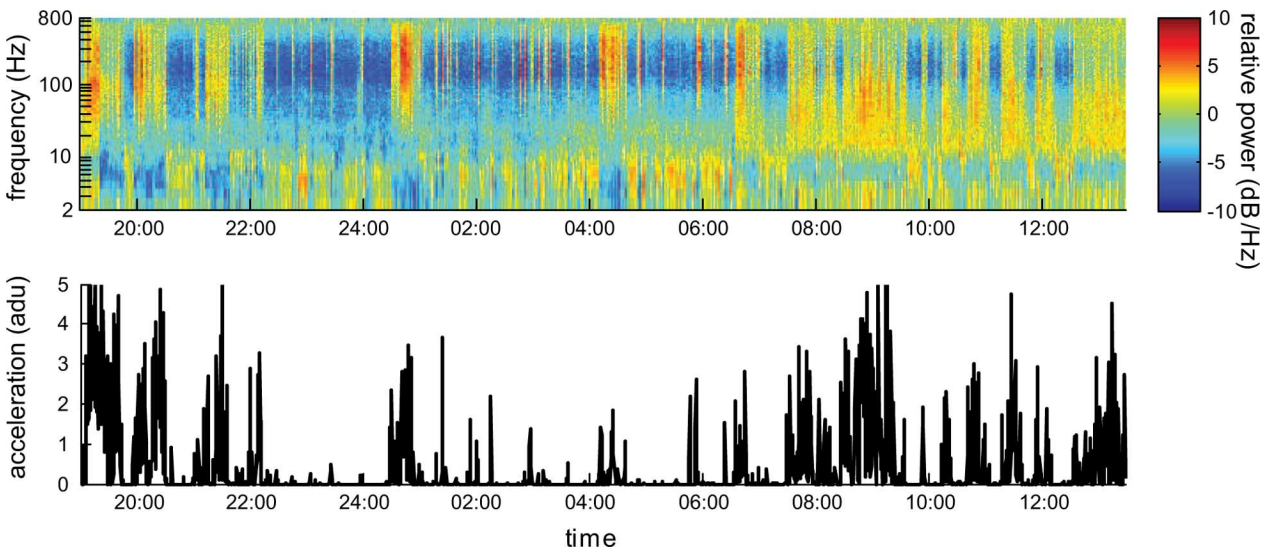

Fig. 6. Eighteen-hour continuous recording of an intracortical local field potential from left motor cortex (top) and right forearm acceleration (bottom). The LFP spectrogram (upper plot) and average acceleration (bottom plot, in digitizer units) were averaged over 30-s bins.

To complement the wider variety of recorded neural signals, the access pins in Neurochip-2 provide a convenient way to interface behavioral monitoring devices, such as an accelerometer. In monkey R, the output of an accelerometer attached to the forelimb was sent to a pair of access pins, and digitized on channel C. Local field potentials (LFPs) in motor cortex were recorded on the other two channels. One of the LFPs is shown in Fig. 6. Again, characteristic sleep-wake cycles were observed in the intracortical field potential. In addition, the recording of the acceleration signal demonstrates a correlation of LFP power changes with movement and rest. In particular, contralateral forearm movement was positively correlated with high-frequency (> 20 Hz) power and negatively correlated with low-frequency (< 10 Hz) power (Fig. 6).

One important new feature of the Neurochip-2 is the ability to stimulate at the high current intensities required for cortical surface and intramuscular stimulation. To illustrate this capability, the HCV version of Neurochip-2 was used to stimulate the surface of the cortex in monkey X during a 24-h session of free behavior in the monkey's home cage. Stimuli were single biphasic pulses (0.2 ms/phase) of 2-mA intensity delivered approximately every 20 s to one of the surface electrodes. EMG activity of the contralateral flexor carpi radialis muscle was continuously recorded at the same time. Stimulus-triggered averages of EMG were then compiled offline for stimuli that occurred during background EMG activity. The normalized averages reveal biphasic motor potentials evoked at a latency of about 10 ms throughout the session. The amplitudes of the average motor potentials were reduced during the night (Fig. 7).

Finally, in addition to stimulating on a fixed schedule as in Fig. 7, stimuli can be delivered contingent on recorded neural events. In one 10-h session with intracortical wire electrodes in

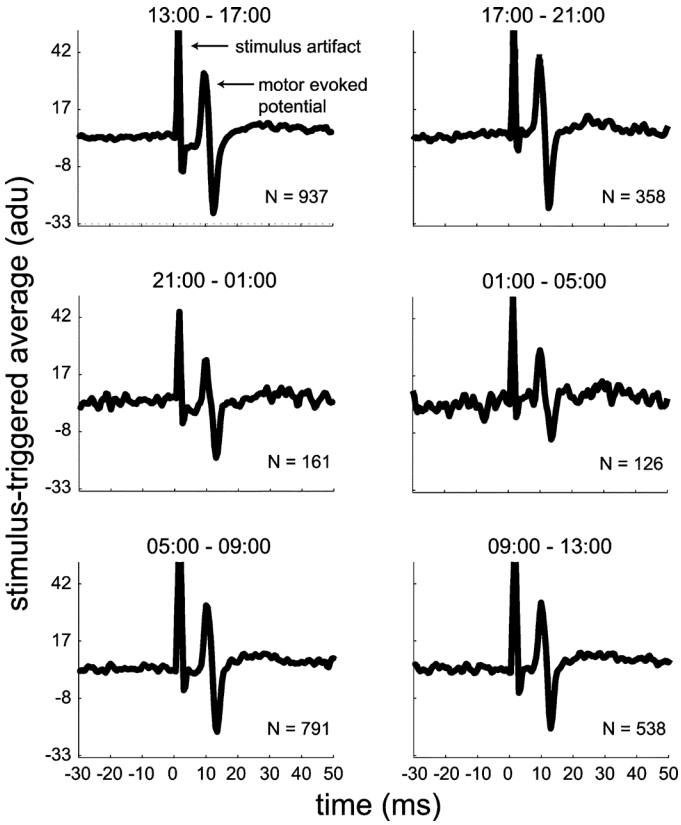

Fig. 7. EMG responses evoked by stimulation of cortical surface using Neurochip-2 (version HCV). Single, biphasic stimuli of 2 mA intensity were delivered every 20 s. Bipolar EMG was continuously recorded from the contralateral flexor carpi radialis muscle. Shown are the average EMG responses during consecutive 4-h-long periods, for stimuli that occurred in the presence of background EMG activity (hence the fewer triggers during night time).

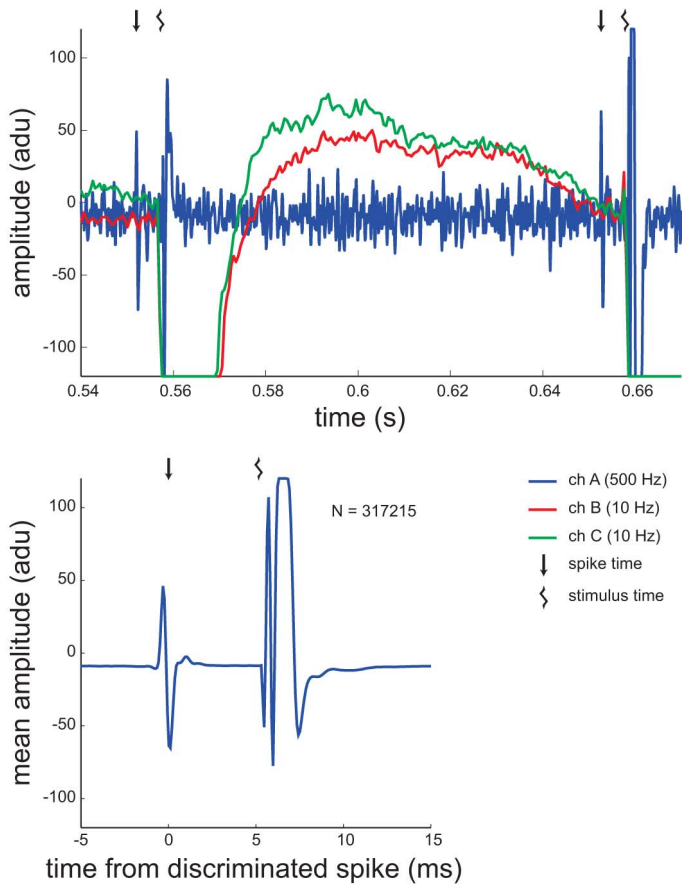

Fig. 8. Closed-loop operation of Neurochip-2. Action potentials were recorded from one intracortical electrode on channel A (500 Hz highpass filter; blue trace) and field potentials were recorded from two other intracortical electrodes on channels B and C (10 Hz highpass filter). The Neurochip was programmed to deliver a 70-μA, 0.2-ms biphasic stimulus pulse to a fourth intracortical electrode 5 ms after each discriminated spike. The experiment ran continuously for 10 h. The top plot shows a short segment of raw data, with two spike-stimulus pairs. The bottom plot shows the average spike waveform and stimulus artifact on channel A. Amplitude in both plots is shown over the full range of digitizer units (adu).

monkey R, the Neurochip-2 was programmed to deliver a stimulus at one site 5 ms after each action potential detected at a second site. In addition, field potentials were recorded from a third and fourth site. Example spike-stimulus pairs are shown in Fig. 8. The 0.4-ms-duration stimulus caused an artifact on the recording channels whose duration was dependent on the high-pass filter cutoff frequency of the channel. The microcontroller can set the amplifier gain to unity during and immediately after stimuli, but this strategy was insufficient to prevent relatively long artifacts with low-frequency recordings (Fig. 8). Thus, only neural events of relatively high frequency (e.g., action potentials or high-frequency LFP power) are well suited to act as triggers in closed-loop operation of Neurochip-2, as low-frequency events would be obscured during the stimulation artifacts. More advanced artifact suppression techniques [21], [22] are being considered for future versions of the device.

V. Concluding Comments

Neurochip-2 is a portable, self-contained system for recording a wide variety of neural and behavioral signals and for delivering electrical stimuli in freely behaving nonhuman primates. Neurochip-2 is designed around programmable PSoC microcontrollers, which have advantages and limitations. The PSoC's 8-bit M8C processor has limited data acquisition capabilities, allowing only a few analog input channels at relatively modest sampling rates. Cypress has recently developed the PSoC-3 and PSoC-5 architectures with more powerful processors that could improve sampling rates and signal resolution, but are still limited to only several analog input channels. The 8 bits used for digitizing the neural signals is lower than the 10–12 bit ADCs used in similar portable devices (e.g., [1]). With the adjustable gain and filter settings we have been able to record either action potentials or field potentials on a single channel, but not both simultaneously. Increasing the ADC resolution is possible with the current system but reduces processing speed, making real-time calculations unfeasible. Thus from strictly a data acquisition viewpoint, the Neurochip-2 has less digitizer resolution and channel count than several recent portable systems optimized for telemetry of multiple channels of data [1], [3], [5], [6].

The strength of the Neurochip is its autonomous recurrent operation without the need for telemetry and the ability to program the PSoC for numerous real-time signal processing scenarios. This makes the Neurochip-2 more than a portable data acquisition system, but rather an embedded computer performing real-time processing operations on inputs, controlling multiple stimulus outputs, and executing programmable contingencies between inputs and outputs. These unique capabilities differentiate

the Neurochip-2 from similar portable devices and empower numerous novel experiments involving autonomously operating real-time recurrent BCIs during free behavior.

ACKNOWLEDGMENT

The authors thank Dr. A. Jackson, Dr. C. Moritz, Dr. S. Perlmutter, Dr. Y. Nishimura, and R. Eaton for helpful suggestions on the design of the Neurochip-2 and on the manuscript. The authors also thank Dr. L. Sorenson for advice on bench testing the Neurochip-2.

Note Added in Proof: A similar system has been described in a paper that appeared after this paper went to press: M. Azin D. J. Guggenmos, S. Barbay, R. J. Nudo, and P. Mohseni, "A Battery-Powered Activity-Dependent Intracortical Microstimulation IC for Brain-Machine-Brain Interface" IEEE J. Solid-State Circuits, vol. 46, no. 4, pp. 731-745, Apr. 2011."

REFERENCES

[1] C. A. Chestek *et al.*, "HermesC: Low-power wireless neural recording system for freely moving primates," *IEEE Trans. Neural Syst. Rehabil. Eng.*, vol. 17, no. 4, pp. 330–338, Aug. 2009.

[2] R. R. Harrison *et al.*, "Wireless neural recording with single low-power integrated circuit," *IEEE Trans. Neural Syst. Rehabil. Eng.*, vol. 17, no. 4, pp. 322–329, Aug. 2009.

[3] H. Miranda *et al.*, "HermesD: A high-rate long-range wireless transmission system for simultaneous multichannel neural recording applications," *IEEE Trans. Biomed. Circuits Syst.*, vol. 4, no. 3, pp. 181–191, Jun. 2010.

[4] R. H. Olsson 3rd *et al.*, "Band-tunable and multiplexed integrated circuits for simultaneous recording and stimulation with microelectrode arrays," *IEEE Trans. Biomed. Eng.*, vol. 52, no. 7, pp. 1303–1311, Jul. 2005.

[5] M. Rizk *et al.*, "A fully implantable 96-channel neural data acquisition system," *J. Neural Eng.*, vol. 6, no. 2, pp. 026002–026002, Apr. 2009.

[6] G. Santhanam *et al.*, "HermesB: A continuous neural recording system for freely behaving primates," *IEEE Trans. Biomed. Eng.*, vol. 54, no. 11, pp. 2037–2050, Nov. 2007.

[7] A. M. Sodagar, K. D. Wise, and K. Najafi, "A fully integrated mixed-signal neural processor for implantable multichannel cortical recording," *IEEE Trans. Biomed. Eng.*, vol. 54, no. 6, pp. 1075–1088, Jun. 2007.

[8] M. Azin *et al.*, "A battery-powered activity-dependent intracortical microstimulation IC for brain-machine-brain interface," *IEEE J. Solid-State Circuits*, vol. 46, no. 4, pp. 731–745, Apr. 2011.

[9] A. Jackson, J. Mavoori, and E. E. Fetz, "Long-term motor cortex plasticity induced by an electronic neural implant," *Nature*, vol. 444, no. 7115, pp. 56–60, Nov. 2006.

[10] A. Jackson *et al.*, "The Neurochip BCI: Towards a neural prosthesis for upper limb function," *IEEE Trans. Neural Syst. Rehabil. Eng.*, vol. 14, no. 2, pp. 187–190, Jun. 2006.

[11] J. Mavoori *et al.*, "An autonomous implantable computer for neural recording and stimulation in unrestrained primates," *J. Neurosci. Methods*, vol. 148, no. 1, pp. 71–77, Oct. 2005.

[12] J. D. Rolston, R. E. Gross, and S. M. Potter, "NeuroRighter: Closed-loop multielectrode stimulation and recording for freely moving animals and cell cultures," in *Proc. IEEE Eng. Med. Biol. Soc. Conf.*, 2009, vol. 2009, pp. 6489–6492.

[13] A. Jackson, J. Mavoori, and E. E. Fetz, "Correlations between the same motor cortex cells and arm muscles during a trained task, free behavior, and natural sleep in the macaque monkey," *J. Neurophysiol.*, vol. 97, no. 1, pp. 360–374, Jan. 2007.

[14] C. T. Moritz, S. I. Perlmutter, and E. E. Fetz, "Direct control of paralysed muscles by cortical neurons," *Nature*, vol. 456, no. 7222, pp. 639–642, Dec. 2008.

[15] S. Venkatraman *et al.*, "A system for neural recording and closed-loop intracortical microstimulation in awake rodents," *IEEE Trans. Biomed. Eng.*, vol. 56, no. 1, pp. 15–22, Jan. 2009.

[16] J. M. Rebesco *et al.*, "Rewiring neural interactions by micro-stimulation," *Frontiers Syst. Neurosci.*, vol. 4, no. 39, pp. 1–15, 2010.

[17] J. D. Rolston, R. E. Gross, and S. M. Potter, "A low-cost multielectrode system for data acquisition enabling real-time closed-loop processing with rapid recovery from stimulation artifacts," *Front Neuroeng.*, vol. 2, pp. 12–12, 2009.

[18] M. Mollazadeh *et al.*, "Micropower CMOS integrated low-noise amplification, filtering, and digitization of multimodal neuropotentials," *IEEE Trans. Biomed. Circuits Syst.*, vol. 3, no. 1, pp. 1–10, Feb. 2009.

[19] R. A. Andersen *et al.*, "Cognitive neural prosthetics," *Trends Cogn Sci*, vol. 8, no. 11, pp. 486–493, Nov. 2004.

[20] A. Jackson and E. E. Fetz, "Compact movable microwire array for long-term chronic unit recording in cerebral cortex of primates," *J. Neurophysiol.*, vol. 98, no. 5, pp. 3109–3118, Nov. 2007.

[21] Y. Jimbo *et al.*, "A system for MEA-based multisite stimulation," *IEEE Trans. Biomed. Eng.*, vol. 50, no. 2, pp. 241–248, Feb. 2003.

[22] E. A. Brown *et al.*, "Stimulus-artifact elimination in a multi-electrode system," *IEEE Trans. Biomed. Circuit Syst.*, vol. 2, no. 1, pp. 10–21, Mar. 2008.

Stavros Zanos received the M.D. degree from Aristotle University of Thessaloniki, Thessaloniki, Greece, in 2000. After completing a three-year residency in Internal Medicine, at the Papageorgiou General Hospital in Thessaloniki, Greece, he joined the Graduate program in Physiology and Biophysics at the University of Washington, Seattle, in 2005. He is currently working towards completing the Ph.D. degree.

Since 2007, he has been a member of the Washington Primate Research Center, Seattle. He is interested in the physiology, technology, and clinical applications of neuroprosthetic devices.

Andrew G. Richardson received the B.S.E. degree in biomedical engineering from Case Western Reserve University, Cleveland, OH, in 2000, and the S.M. degree in mechanical engineering and the Ph.D. degree in biomedical engineering from the Massachusetts Institute of Technology (MIT), Cambridge, in 2003 and 2007, respectively.

He was a Postdoctoral Associate at MIT in 2007–2008 and is currently a Senior Fellow at the University of Washington, Seattle. His research interests include motor learning, neuroplasticity, and neuromodulation.

Larry Shupe received the B.S. degree in computer science from the University of Washington, Seattle, in 1986.

He currently works as an Information Technology Specialist in the Department of Physiology and Biophysics at the University of Washington.

Frank P. Miles received the B.S. degree in electrical engineering from Rochester Institute of Technology, Rochester, NY in 1975, and the M.S., M.S.E.E, and Ph.D. degrees in bioengineering from the University of Michigan, Ann Arbor, in 1982, 1983, and 1986, respectively.

He is currently a Research Scientist/Engineer at the University of Washington, Seattle. His interests include stimulator design for optimal electrode potential recovery.

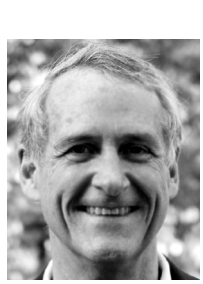

Eberhard E. Fetz received the B.S. degree in physics from the Rensselaer Polytechnic Institute, Troy, NY, in 1961, and the Ph.D. degree in physics from the Massachusetts Institute of Technology, Cambridge, in 1966.

He is currently Professor of Physiology and Biophysics and Adjunct Professor of Bioengineering at the University of Washington, Seattle. He is also a Core Staff member of the Washington National Primate Research Center, Seattle. His primary research interest is neural mechanisms of volitional control of limb movements in behaving primates. His current research is focused on applications of bidirectional implantable BCIs.